Sediment Thickness and Moho Depth Beneath Western Indonesian Region From Teleseismic Receiver Function

Syaiful Bahri
Universitas Gadjah Mada
Wiwit Suryanto (ws@ugm.ac.id)
Universitas Gadjah Mada Fakultas Matematika dan Ilmu Pengetahuan Alam https://orcid.org/0000-0002-6275-7880
Drajat Ngadmanto
BMKG: Badan Meteorologi Klimatologi dan Geofisika

Full paper

Keywords: teleseismic receiver function, sediment thickness, Moho depth, Western Indonesia Region

Posted Date: March 31st, 2021

DOI: https://doi.org/10.21203/rs.3.rs-356661/v1

Abstract

The Earth's crust layer and sediment in Western Indonesia has been studied using the inversion of teleseismic receiver function from BMKG's seismic network. Earthquake events were analyzed in this study with a moment magnitude greater than 6.0 with epicentral distances of 30° to 90°. A total of 60 earthquake events were observed and recorded by 91 stations around the study area. Furthermore, an inversion process was carried out using the initial velocity model from the modification of the AK135f velocity model to obtain the shear wave velocity structure below each stations. The velocity model from the azimuthally stacked vertical receiver function showed that the sediment layer had a relatively medium shear wave velocity value with an average of 2.1 km/s, while the crust layer had 4.60 km/s. The sedimentary layer thickness in this region also varies between 2 km to 10 km. A relatively thick sediment layer of about 8 km to 10 km was observed in two locations, in East Kalimantan associated with the Kutai Basin and Northern part of Sumatera in the North Sumatera Basin, a two major oil producer basinal area in Indonesia. The Moho discontinuity was also found at depths that vary between 16 km to 50 km. In addition, the most shallow Moho depth is 16 km below the North Kalimantan and North part of West Java, while the deeper Moho depth of 50 km is located below East Kalimantan, Central Kalimantan, North Sumatera and South Sumatera.

1. Introduction

Indonesia is part of the Eurasian plate, bordering the Indo-Australian plate in the south and the Pacific plate in the east. The tectonic mechanism divides Indonesia into two regions, namely the western and eastern parts which formed in the Mesozoic to Cenozoic era. They were formed based on the process of directional change and rate of movement of the tectonic plates. During the Jurassic to late Cretaceous period, active tectonics resulted in plate movement from the Malay Peninsula area in mainland Asia, as well as large islands such as Sumatera, Kalimantan and Java to other small islands, this plate is called the Sundaland (Hall, 2009).

Sundaland tectonics is part of the Eurasian plate located in western Indonesia. The tectonic development experienced the Indo-Australian plate collision under the Sundaland plate which resulted in the Sunda Arc area that stretches from Sumatera, Java, to the island of Sumbawa (Soeria-Atmadja et al., 1998). The activity of continuous plate convergence up to the present time affects the formation of complex geological structures.

Western and Eastern Indonesia are separated by the islands of Kalimantan and Sulawesi with a complex structure, which is also a transitional area between the peculiarities of the geological features of the Asian and the Australian continent. Previous studies on crustal structure have been carried out in Indonesia using the receiver function method, including in the island of Sumatera, where the thickness of the earth's crust varies from 16 km to 40 km (Kieling et al., 2011; Macpherson et al., 2012; Bora et al., 2016). Other researchers performed the receiver function study in the island of Java where the thickness of the crust in the western part of the island was 25–37 km (Syuhada and Anggono, 2016; Anggono et al.,

2020), in the central and east part of Java island about 25–39 km (Wölbern and Rümpker, 2016; Amukti et al., 2019). Recently, the receiver function study using limited number of stations in Borneo or Kalimantan Island was carried out by Bahri et al., 2021. They showed the evidence of thickening of the Earth's crust in cross-section from east Java to the north to Borneo Island.

However, information on sediment layer thickness and the Moho depth for western Indonesia is still limited, especially in Kalimantan and Bali. In this study, the receiver function was used to model the structure under the observation station using a three component seismometer (Herrmann et al., 2001; Suryanto et al., 2010) for all available seismic stations belonging to the Meteorology, Climatology, and Geophysical Agency (BMKG) of Indonesia. This research is very important, both for the purposes of earthquake disaster mitigation and for the precise determination of earthquake hypocenter. It also establishes practical purposes in the development of oil and gas exploration in western Indonesia.

2. Geology Setting

Tectonic evolution has provided an overview for the geological history of western Indonesia. This can be explained by the arrangement and age of the rocks in the area. Tectonic interactions result in complex geological conditions in the presence of troughs, non-volcanic outer arcs, volcanic, arc basins and back arcs. This study obtained geological information based on the area of the sediment basin for the islands of Sumatera, Java, Bali and Kalimantan. The formation of sedimentary basins was closely related to the movement of the crust from the tectonic processes experienced by the plates.

The area of the sedimentary basin in western Indonesia is shown in Fig. 1. This map is based on gravity and geological data. The classification of basins based on age is divided into two, namely tertiary and pre-tertiary basins. Based on the tectonic arrangement, the basins are further divided into 11, namely back-arc, intermontane, fore-arc, trench, foreland, passive margin, oceanic basins, deltaic basins, rifting valley, transtensional, and transtensional marginal oceanic basin. Based on recent geology and geophysics information, Satyana et al. (2012) found about 86 basins with 16 producing oil/gas, 7 discoveries based on well data, and 25 with hydrocarbon indication from well data, 37 without current discoveries and 4 without seismic data. (Geological Agencies of Indonesia, 2009).

3. Data Set

This study utilized seismogram data from the global network belonging to Indonesia's BMKG (IA Network). Each station had a three-component broadband type seismometer sensor operated by BMKG and supported by GFZ-Potsdam Germany with 91 stations spread across Sumatera, Java, Bali and Kalimantan (Fig. 2).

The earthquake events were selected with the criteria of a moment magnitude > 6.0, with an epicentral distance of 30°-90° (teleseismic event). The early stage of the processing involved the addition of header parameters to the raw data, such as the coordinates of the earthquake source information, the origin time,

and the magnitude of the earthquake. A further processing step included the instrument correction to produce the true ground motion in units of m/s (Herrmann, 2013).

4. Methodology

In the first step of data processing, the rotation from the cartesian coordinate system (X,Y,Z) to the radial component was performed using a simple 2D rotation of coordinate transformation, converting two horizontal components into radial (R) and transverse (T) components. The Z,R,T data were then windowed using a time window of about 10 seconds before the arrival time of the P-wave and 30 seconds after the arrival time of the P-wave, with the conversion phase of the Ps-wave appearing. Furthermore, the receiver function calculation involved an iterative time-domain deconvolution technique (Ligorría and Ammon, 1999) using a Gauss filter parameter at a width of 2.5 and a limit of 500 iterations. In this study, the response in the radial direction was selected because the Ps-wave response in Moho was seen to be the greatest in its waveform. The response receiver function in the radial direction of each earthquake was selected for the best (showing the same wave phase response in each earthquake) and then stacked altogether (Fig. 3).

Receiver function inversion calculation utilized the standard receiver function code developed by Herrmann and Ammon (2004). Inversion calculations were carried out to obtain a model of the S-wave velocity below the station (Fig. 4). The inversion process was based on an initial velocity model modified from the AK135f velocity model developed by Kennett et al. (1995). Furthermore, the observed data were in form of stacks of waves at each station. As many as 15 iterations were limited until a match between the response of the prediction model and the observational data related to a minimum of their misfit.

5. Results And Discussion

5.1 Receiver function response

In general, the location of seismic stations in Sumatera Island lies in various basinal areas and tectonic setting. About 41 stations had a receiver function waveform with a characteristic of the P-wave at 0–0.5s (Fig. 5.a), the converted P-S at 1.0 s and 2.5 related with the sediment layer below the station, which is also called the Pss sediment phase. This station was associated with the geological environment of the sedimentary basin on the island of Sumatera. In addition, phase amplitude at 3.0 to 5.5 s were assumed to be the Ps-waves from Moho, and multiple (PpPs) indicated in signals from 12.0 to 16.0 s.

In Java Island, about 34 seismic stations were observed. These stations are associated with a basinal area classification consisting of back-arc in the northern part of Java, fore-arc in the south, and Intermontane basin. The resulting stack receiver function calculation is shown in Fig. 5.b. On average, the wave response showed a 0-0.5 s signal presumably in the P-wave phase. The 1.0–2.0 s signal represents a conversion of the Sediment Pss wave. Signal at 11.5 s and 15.0 s was predicted to have a PpPs wave phase for Ps 3.0 s and Ps 5.0 s, respectively.

Figure 5.c is a stack receiver function at an earthquake observation station on the island of Bali. These stations are in form of SRBI, KHK, RTBI, IGBI and DNP which are located on a surface composed of various rocks from volcanic products (Geiger et al., 2018; Igan, 2009). The island of Bali is flanked by two sedimentary basins, specifically the fore-arc and back-arc. Furthermore, the average wave response at this station had a complex shape at a 0–3.0 s signal. The Ps Moho phase was believed to have been converted in the signal range 3.0-5.5 s while the PpPs phase was converted in the range 11.5–15.5 s.

The wave response at the BMKG station on Kalimantan island is shown in Fig. 5.d. There were 11 seismic stations occupying various sedimentary basins in the region. This island is located in the classification of basins that are tertiary and pre-tertiary, also located in the arrangement of back-arc basin, foreland, trench, passive margin, and deltaic basin. The average wave stack showed a P-wave response to a 0-0.5 s signal, Pss Sediment was converted to a 1.5-2.0 s signal, Ps Moho was converted to a 3.0-4.5 s signal, and multiple waves PpPs converted in the range 11.5–15.5 s.

5.2 S-wave velocity models in variations in the depth of the Earth

The S-wave velocity modeling was obtained from the inversion results at each station in Western Indonesia, as shown in Fig. 6. This model produced an S-wave velocity value within 1.00 km/s to 6.80 km/s range which was illustrated with a color scale for each variation of the earth's depth. This Vs velocity value interpolation was made using the gridding method (Smith and Wessel, 1990) algorithm with an interval of 0.1° for variations in velocity values at each station. For a depth of 2 km, the velocity model obtained an average velocity value of about 2.10 km/s which dominated the stations in Western Indonesia, except for TRSI stations with a velocity value of 5.10 km/s. The category for the Vs velocity value at 2 km depth was the very low S-wave velocity from the earth's surface. Meanwhile, 6 km depth experiences changes in velocity Vs which varied with an average of about 3.00 km/s and several areas which showed large velocities ranging from 4.00–5.00 km/s. These were observed in Central Sumatera, South Java and Central Kalimantan.

A depth of 10 km showed the value of the velocity which varied with an average of 3.40 km/s spread under the stations. Meanwhile, a large Vs velocity value was also observed at a range of 4.50–6.40 km/s in several areas such as Central Sumatera (station TRSI, BKNI, SBSI, and RGRI), Southern Sumatera (station SLSI, KLI and LWLI), West Java (station SBJI), South side Java (station YOGI and KRK), North side Java (station UWJI and BWJI), and Central Kalimantan (station PKKI and PBKI). Some low velocity values of about 2.00 km/s were also observed in the area of East Kalimantan and northern Sumatera. A depth of 16 km results in a change in velocity that is not significant, different from a depth of 10 km, with an average velocity value of 3.50 km/s for the observation station.

For depths of 20 km and 26 km, the velocity model began to experience a greater change in the value of Vs below each station. At 20 km, the velocity model was obtained with an average value of Vs velocity 3.60 km/s. Meanwhile, the depth of 26 km experienced a change in Vs with an average value of 3.80 km/s which was spread under the observation station.

For depths of 30 km to 40 km, the results of this modeling showed that the change in the value of Vs dominated the range of 4.00-4.60 km/s. The greatest value of Vs velocity ~ 6.68 km/s was the result of inversion calculations from data from the RTBI station on the island of Bali, located at a depth of 30 km. Variations in depth of 46 km, 50 km, and 56 km experienced changes in the value of Vs velocity ranging from 4.20-5.00 km/s which are spread across all stations in Western Indonesia. The velocity model category at this depth variation was a large value for the velocity Vs to obtain the layer information in the earth's crust. This research limits to a depth of 56 km for the Vs velocity modeling because this velocity change does not experience a significant difference in any of these depth variations.

The characteristics of the sedimentary layer were characterized by a low S-wave velocity from the earth's surface and the Moho discontinuity limit indicated by a sudden large change in velocity Vs from the crust to the earth's mantle. This research limits the velocity value of Vs to 4.50 km/s for the velocity of the Earth's mantle. The results of the S-wave velocity model produced an average Vs value for the sediment layer of 2.10 km/s and 4.60 km/s for the earth's crust.

5.3 Variations of Sediment Thickness and Moho Depth in Western Indonesia

Figure 7 shows a map of variation of sediment thickness in Western Indonesia. The interpretation of the sediment layer and Moho obtained from the S-wave velocity model correlated with geological information. Therefore, the results showed that the sediment layer throughout Western Indonesia varies from a thickness of 2 km to 10 km. This sediment layer is relatively thick, between 6–10 km and lies beneath the regions of East Kalimantan, East Java, northern Central Java and northern Sumatera. The variation in the thickness of the sediment layer is influenced by geological conditions at each position of the seismic station.

Kalimantan is an area with a tertiary and pre-tertiary basin zone. However, the BMKG network station is in a tertiary basin area. Satyana et al. (1999) stated that the estimated thickness of tertiary sediments in Kutai Basin is 10–11 km, in Barito Basin is 4 km and the Tarakan Basin is 9 km. In addition, information on sediment thickness of ~ 2 km can be found in areas such as Asam-Asam, Melawi, and Ketungau-Mandai basins (Hall and Nichols, 2002). This study showed that the sediment layer for the island of Kalimantan is dominated by a thickness of 2 km, except under the East Kalimantan area associated with the Kutai Basin (BKB, SMKI, and SGKI stations) with a thickness of 6–10 km (Fig. 7). Therefore, the sediment layer thickness estimates from this study had results consistent with the geological survey.

The basin area in Sumatera is divided into two major parts, namely the fore-arc and back-arc. The results showed that the average sediment layer in this area was estimated to be about 2 km thick except for Nias Island (GSI Station) and Sinabang Island (SNSI Station) which correlated with the front arc basin, as well as Northern Sumatera (LHMI and LASI stations) and Sumatera. Furthermore, the southern part (JMBI station) is associated with the back-arc basin which has a sediment thickness ranging from 6–8 km. This result is supported by several other researchers, namely Moore et al. (1982) which estimated that the average sediment thickness in the Sumatera front arc zone is 4–6 km. Additionally, the tertiary sediment

data information for the back arc basin in the North Sumatera basin had a sediment thickness of 6 km (Wicaksono et al., 2009), Central Sumatera had a sediment thickness range of 2.5 to 3.0 km (Cahyaningsih et al., 2018), and The South Sumatera basin was also estimated to have a sediment thickness of 4–7 km (De Coster (1974) in the Lemigas Team, (2017)).

In other islands, this study also found a sediment thickness that varies from 2 km to 6 km in the Java region. The thickest sediment, which was 6 km, is found in the Central Java area in the northern part and East Java associated with the Kendeng sedimentary basin (SMRI and ABJI stations) and the North East Java (KMMI) basin. Meanwhile the thickness of other basins was found to be about 2 km from the surface of the earth. The geological survey results estimated that the area of the northwest Java basin, Bogor basin, and the southern ridge sediment thickness was above 2 km (Satyana, 2005). In another study, the tomography method resulted in sediment thickness ranging from 8–10 km which is located under the Kendeng and Rembang geological zones in East Java area (Martha et al., 2017).

Bali is a small island with a tertiary age sedimentary basin known as North and South Bali-Lombok basin. Geological research showed that the Bali-Flores Basin, located on the southeastern edge of the Sunda Shield, estimates its sediment thickness from 1 km to 2 km (Prasetyo, 1992). Geological study also shows that the results are similar to this study, and the sediment thickness of 2 km were found under the island of Bali.

Figure 8 is a map of the depth variation for the Moho discontinuity in Western Indonesia. This study resulted in depths varying from 16 km to 50 km for the Moho discontinuity. Meanwhile, in Kalimantan region, Moho was found at a relatively shallow depth, specifically between 16–20 km in the southern part (station BBKI and KBKI) and the northern part (station TARAI). Moho also had the deepest depth, about 50 km located in Central Kalimantan (station PBKI) and East Kalimantan (station SMKI). In other areas, Java and Bali, the Moho depth varies with an average depth of about 36 km, except for Southern Java which is associated with the geological environment of the Southern Mountains (station SKJI and KRK). Northern West Java which correlates with the Bogor zone and the North West Java basin (station DBJI, TNG and JCJI), as well as northern East Java which correlate with the Rembang zone (station GRJI) had a depth of 16–26 km. In Sumatera Island, the Moho depth varies with an average of about 34 km, but a relatively shallow depth of 20 km is found in the border area of Central and South Sumatera which has implications for the fore-arc basin (station MNAI, KLSI, KRJI, and PBSI) > In addition, most within about 50 km are found beneath North and South Sumatera areas associated with the back-arc basin (station KCSI and PMBI).

The variation in sediment thickness and Moho depth from the results of previous and present studies on the islands of Sumatera and West Java are shown in Table 1 and Table 2, respectively. In other areas, Central and East Java had Moho discontinuity depth ranges from 25–39 km (Wölbern and Rümpker, 2016; Amukti et al., 2019). Meanwhile, current research estimated Moho's depth in the area to be 20–46 km.

Laske et al. (2013) published a global model for sediment layer thickness and Moho depth called CRUST 1.0. The modeling results showed that the thickness of the sediment layer varies from 1 km to 8 km with the thickest sedimentary layer, located 8 km below East Kalimantan which is associated with the Kutai Basin. Furthermore, this model also produced a sediment layer with a thickness of 4 km located in Central Kalimantan which correlates with the Barito Basin and the East Java area associated with the North East Java and Kendeng basins, while the other areas are dominated by a thickness of about 1–2 km. This model showed results consistent with that of current research, namely that the thickest sediment layer is about 6 to 10 km in East Kalimantan, East Java, northern Central Java and northern Sumatera. The Moho discontinuity depth of the CRUST 1.0 model ranged between 25 km to 32 km in Western Indonesia. This modeling also found that the Moho depth beneath the island of Kalimantan is deeper than that of Sumatera, Java and Bali. The relatively shallow depth of Moho, between 25–28 km, is located in the southern part of Sumatera-Java-Bali. Meanwhile, the results of current research showed that Moho's depth varies from 16 km to 50 km and Moho in the southern part of Sumatera-Java-Bali had a depth between 20 km to 40 km.

Other geophysical research methods have been investigated for the Moho discontinuity boundary in several parts of Western Indonesia. This research method involved refraction seismic methods, gravity survey and tomography. One of them is the boundary of the North and Central Sumatera region which correlates with the geological area of the front and back arc basins, where the Moho discontinuity boundary is at a depth of 30 km (Kieckhefer et al., 1980; Simoes et al., 2004; Lange et al., 2018). The correlation of previous studies showed consistent results with current studies that Moho discontinuities are also found at depths between 30 km to 40 km in the border areas of North and Central Sumatera (GSI and TDNI, PSI and TRSI stations). The southern part of Java and Bali also had Moho depths ranging from 18–25 km (Curray et al., 1977), and current research estimates Moho to be between 30km to 46 km depth.

5.4 High Velocity Layer

The high velocity layer is the result of the S-wave velocity model which underwent a large change in wave velocity from the surface to a depth of 10 km. Figure 9 is a distribution map for the HVL zone. The HVL category of this research was in the form of S-wave velocity values of 4.00-6.50 km/s for the top layer (surface) to the layer at a depth of 10 km below the Central Kalimantan, Java and Central to Southern parts of Sumatera.

The Central Kalimantan area had the HVL zone under three receiving stations. Based on geological information, Central Kalimantan is an area associated with the Barito Basin where there are bedrock types in form of metamorphic rocks at a depth of 4 km to 7 km (Satyana et al., 1999; Darman, 2017). In addition, this area also has a sedimentary basin called Pembuang, with the bedrock located at a depth of 2.5 km. These bedrock in form of igneous and metamorphic rocks form a higher topography and limit the Pembuang basin in the west-northwest part of Kalimantan (Badan Geologi, 2009). Therefore, this HVL is believed and interpreted as a metamorphic rock at a depth of 6–10 km below the station PBKI, PKKI and MTKI.

The Java area has several stations that produce large wave velocity from a depth of 6 km to 10 km. Hard bedrock were suspected to be present at each station. One of them is the station SBJI which is associated with the geological area of the quaternary volcano, as indicated by the presence of Banten tuff rocks (Henda, 2018). Station CNJI and KRK stations are located in the geological environment of the Southern Mountains which consists of volcanic deposits of old andesites formed in the Miocene era. Furthermore, the YOGI station is located in the geological area of the Central Java Depression with the Old Andesite Formation formed in the Oligo-Miocene era. Station UWJI is also associated with a quaternary volcanic environment consisting of andesite or basalt rocks (Satyana, 2005). In addition, the station BWJI is located in the Bawean basin area where there are igneous or intrusive rock types (Manur and Barraclough, 1994).

Another area, Sumatera, also has an HVL zone below the station which is associated with the geological area of the forebear and back arc basins. The TRSI station is located in the Southern Mount area which produces large wave velocities, which are possibly hard rock exposed on the surface. Meanwhile, along the Barisan Mountains area, there is also HVL at a depth of 6 km and 10 km. The Barisan Mountain was formed from tectonic activity which caused all sedimentary rock to fold and grow strongly, followed by volcanism allowing the bedrock to be lifted to the surface. Macpherson et al. (2012) and Bora et al. (2016) believed that the HVL under the BKNI station is due to a layer of sedimentary rock overlapping the bedrock in the back-arc basin area. From geological information, the rock characters scattered on the island of Sumatera are volcanic, including the igneous rock type consisting of andesite and diorite found in Lampung (Indarto et al., 2008).

Therefore, it is believed that HVL in Western Indonesia is interpreted for bedrock layers in form of igneous or metamorphic rock types. The HVL response produced a relatively deeper Moho discontinuity. This is indicated by the response of wave velocity under station PBKI (Kalimantan) and station PMBI (Sumatera) at a depth of up to 50 km.

5.5 Earthquake Hazard Scenarios in Western Indonesia Region

Western Indonesia has the subduction of the Indo-Australian plate into Eurasia which results in earthquakes of large magnitude occurring frequently. Large-scale earthquake events have occurred in the Aceh, Nias, Bengkulu, Mentawai, Pacitan and Pangandaran areas with a moment magnitude > 7.0 (National Earthquake Study Center Team, 2017). The USGS data stated that earthquakes often occur in the southern Sumatera-Java-Bali subduction zone with a moment magnitude > 5.0 in 2010–2020.

One contribution from the results of the receiver function is that it can be used as an earthquake hazard scenario from the information on sediment layer thickness and the depth of the Moho discontinuity limit shown in Fig. 10. Earthquakes of large magnitude can cause tsunamis, huge casualties and loss of property in parts of the southern coastal zone. Information on sediment thickness and Moho depth followed by large earthquake activity can make it more vulnerable to earthquake hazards, especially in the southern part of Sumatera-Java-Bali. Furthermore, there are relatively safe areas from earthquake

hazards, namely Kalimantan, as this area is far from the subduction zone, and there are fewer earthquakes.

6. Conclusion

From the results of this study, the following conclusions can be drawn:

a. The average response receiver function produced a sediment-Pss wave response from a signal of 1.0 s to 2.0 s, Ps Moho phase is in the signal range 3.0–6.0 s and multiple (PpPs) is converted to signal 12.0–16.0 s under Kalimantan, Sumatera, Java, and Bali.
b. The S-wave model obtained from the calculation showed a variable velocity value for each station, with an average Vs of 2.10 km/s for the sediment layer and 4.60 km/s for the crust layer.
c. In Western Indonesia, the thickness of the sediment layer and the Moho depth varies. The sediment layer ranges in thickness variations from 2 km to 10 km with a relatively thick layer of about 8–10 km. There are two locations, namely East Kalimantan associated with the Kutai Basin, and northern Sumatera which correlates with the North Sumatera sedimentary basin. Moho discontinuities were also found at depths ranging from 16 km to 50 km. The shallowest Moho depth of ~ 16 km was found under the North Kalimantan area which corresponds to the geological zone of the Tarakan basin and northern West Java which correlates with the North West Java basin. Meanwhile, the deepest ~ 50 km was found under East Kalimantan, Central Kalimantan, North Sumatera, and South Sumatera.

Abbreviations

BMKG : Badan Meteorologi Klimatologi dan Geofisika (Indonesian Meteorology, Climatology and Geophysical Agency), GFZ: GeoForschungs Zentrum Germany, HVL: High Velocity Layer, IA : FDSN Code for InaTEWS Indonesia Tsunami Early Warning System.

Declarations

Availability of data and materials

The data is maintained by the Agency of Meteorology, Climatology and Geophysics of Indonesia (BMKG) and will be available upon requests to the Agency.

Competing interests

The authors declare that they have no competing interests.

Funding

This research was funded by the RTA, Thesis Recognition Program Nr. 2488/UN1.P.III/DIT-LIT/PT/2020, from Universitas Gadjah Mada granted to WS.

Authors' contributions

SB contributed to the data analyses, and manuscript preparation. WS contributed data analyses and editing the manuscript. DN contributed to the data preparation and analyses. All authors read and approved the final manuscript.

Acknowledgements

This research is part of the first's author Master Project at the Post Graduate Master Program in Physics, Universitas Gadjah Mada. The authors express their gratitude to Prof. Robert B Hermann, for the Fortran Code. All of the figures were rendered using the Generic Mapping Tool.

References

1. Amukti, R., Yunartha, N.A., Anggraini, A., and Suryanto, W., 2019. Modeling of The Earth's Crust and Upper Mantle Beneath Central Part of Java Island Using Receiver Function Data, AIP Conference Proceedings, Vol, 2194, No. 1, pp 020004, https://doi.org/ 10.1063/1.5139736.
2. Anggono, T., Syuhada, S., Febriani, F., Handayani, L., Mukti, M.M. and Amran, A., 2020. Crustal shear-wave velocity structure in Western Java, Indonesia from analysis of teleseismic receiver functions. *Journal of Earth System Science*, Vol.129, No. 6, pp. 1-22, https://doi.org/10.1007/s12040-019-1288-1.
3. Badan Geologi. 2009. *Peta Cekungan Sedimen Indonesia*. <*https://geology.esdm.go.id/cekungan/*>
4. Bahri S., Suryanto W., and Ngadmanto D, 2021 Sediment and Crustal Structure Beneath East Kalimantan and East Java, Indonesia From Receiver Function, *J. Phys.: Conf. Ser.* 1825 012014, doi:10.1088/1742-6596/1825/1/012014
5. Bora, D.K., Borah, K. and Goyal, A., 2016. Crustal shear-wave velocity structure beneath Sumatera from receiver function modeling. *Journal of Asian Earth Sciences*, Vol. 121, pp. 127–138, http://dx.doi.org/10.1016/j.jseaes.2016.03.007.
6. Cahyaningsih, C., Crensonni, P.F., Aditia, Y., Suryadi, A., Yuskar, Y., Choanji, T., Putra and Dewandra, B.E., 2018. Petrography, Geology Structure and Landslide Characterization of Sumatera Fault Deformation: Study Case In Km 10-15 Highway, Koto Baru Sub District, West of Sumatera. *Journal of Geoscience, Engineering, Environment, and Technology*, Vol. 3, No. 04, pp. 192-199, https://doi.org/10.24273/jgeet.2018.3.4.2062.
7. Curray, J.R., Shor, G.G., Raitt, R.W. and Henry, M., 1977. Seismic refraction and reflection studies of crustal structure of the Eastern Sunda and Western Banda Arcs. *Journal of Geophysical Research,* Vol. 82, No. 17, pp. 2479–2489, https://doi.org/10.1029/JB082i017p02479.

8. Darman, H., 2017. The Paleogene of East Borneo and its Facies Distribution. *Berita Sedimentologi*, Vol. 1, No. 37, pp. 5–13.
9. De Coster, G.L., 1974. The Geology of the Central and South Sumatera Basins. *Proceeding of third Annual Convention of Indonesian Petroleum Association*, pp. 77-110.
10. Geiger, H., Troll, V.R., Jolis, E.M., Deegan, F.M., Harris, C., Hilton, D.R. and Freda, C., 2018. Multi-level magma plumbing at Agung and Batur volcanoes increases risk of hazardous eruptions. *Scientific Reports*, Vol. 8, No. 10547, pp. 1–14, https://doi.org/10.1038/s41598-018-28125-2.
11. Hall, R. and Nichols, G., 2002. Cenozoic sedimentation and tectonics in Borneo: Climatic influences on orogenesis. *Geological Society Special Publication*, Vol. 191, pp. 5–22, https://doi.org/10.1144/GSL.SP.2002.191.01.02.
12. Hall, R., 2009. Indonesia, Geology. in R Gillespie and D Clague (eds), *Encyclopedia of Islands.* University of California Press, Berkeley, California, pp. 454-460.
13. Henda, T. 2018. Rawa Dano; Sebuah Kaldera Gunung Api Purba. Dinas Energi dan Sumber Daya Mineral Provinsi Banten. <*https://desdm.bantenprov.go.id/read/berita/283/RAWA-DANO-SEBUAH KALDERA-GUNUNG-API-PURBA.html*>.
14. Herrmann, R.B., Ammon, C.J. and Julia, J., 2001. Application Of Joint Receiver-Function Surface-Wave Dispersion For Local Structure In Eurasia. *Proceedings of the 23rd Seismic Research Review: Worldwide Monitoring of Nuclear Explosions*, pp. 46–54.
15. Herrmann, R.B. and Ammon, C., 2004. *Surface waves, receiver functions and crustal structure, Computer programs in Seismology, Version 3.30*. ed. Department of Earth and Atmospheric Sciences Saint Louis University.
16. Herrmann, R.B., 2013. Computer programs in seismology: An evolving tool for instruction and research. *Seismological Research Letters,* Vol. 84, No. 6, pp. 1081–1088, https://doi.org/10.1785/0220110096.
17. Igan, S.S., 2009. Ignimbrite Analyses of Batur Caldera, Bali , based on ^{14} C Dating. Indones. *Jurnal Geologi Indonesia,* Vol. 4, No. 3, pp. 189–202.
18. Indarto, S., Zulkarnain, I., Setiawan, I., Fauzi, A., Listiyowati, L.N. and Yuniati, M.D., 2008. Monografi Batuan Volkanik Di Sayap Barat Pegunungan Bukit Barisan, Sumatera Aplikasinya Dalam Ilmu Kebumian. *Prosiding Pemaparan Hasil Penelitian Puslit Geoteknologi*, pp. 978–979.
19. Kennett, B.L.N., Engdahl, E.R. and Buland, R., 1995. Constraints on seismic velocities in the Earth from traveltimes. *Geophysical Journal International*, Vol. 122, pp. 108–124, https://doi.org/10.1111/j.1365-246X.1995.tb03540.x.
20. Kieckhefer, R. M., Sho, G. G. and Curray J. R., 1980. Seismic refraction studies of the Sunda trench and forearc basin. *Journal Of Geophysical Research*, Vol. 85, No. B2, pp. 863-889.
21. Kieling, K., Roessler, D. and Krueger, F., 2011. Receiver function study in northern Sumatera and the Malaysian peninsula. *Journal of Seismology*, Vol. 15, pp. 235–259, https://doi.org/10.1007/s10950-010-9222-7.

22. Lange, D., Tilmann, F., Henstock, T., Rietbrock, A., Natawidjaja, D. and Kopp, H., 2018. Structure of the central Sumateran subduction zone revealed by local earthquake travel-time tomography using an amphibious network. *Solid Earth,* Vol. 9, pp. 1035–1049, https://doi.org/10.5194/se-9-1035-2018.
23. Laske, G., Masters, G., Ma, Z. and Pasyanos, M., 2013. Update on CRUST1.0-A 1-degree Global Model of Earth's Crust. Geophysical Research Abstracts, <*https://igppweb.ucsd.edu/~gabi/crust1.html*>.
24. Lemigas Team, 2017. Geological Setting Of South Sumatera Basin (Shale Hidrocarbon Basins In Indonesia. Research And Development Center For Oil And Gas Technology "Lemigas", Agency Of Research And Development For Energy And Mineral Resources, Ministry Of Energy And Mineral Resources Republic of Indonesia, <*http://ccop.asia/uc/data/43/docs/Indonesia-UCM7.pdf*>.
25. Ligorría, J.P. and Ammon, C.J., 1999. Iterative deconvolution and receiver-function estimation. *Bulletin of the Seismological Society of America*, Vol. 89, No. 5, pp. 1395–1400.
26. Macpherson, K.A., Hidayat, D. and Goh, S.H., 2012. Receiver function structure beneath four seismic stations in the Sumatera region. *Journal of Asian Earth Sciences*, Vol. 46, pp. 161–176, https://doi.org/10.1016/j.jseaes.2011.12.005.
27. Manur, H. and Barraclough, R., 1994. Structural Control On Hydrocarbon Habitat In The Bawean Area, East Java Sea. *Proceedings Indonesian Petroleum Association Twenty Third Annual Convention*, pp. 129–144.
28. Martha, A.A., Cummins, P., Saygin, E., Sri Widiyantoro, and Masturyono, 2017. Imaging of upper crustal structure beneath East Java–Bali, Indonesia with ambient noise tomography. *Geoscience Letters*, Vol. 4, pp. 1–12, https://doi.org/10.1186/s40562-017-0080-9.
29. Moore, G.F., Curray, J.R. and Emmel, F.J., 1982. Sedimentation in the Sunda trench and forearc region. *Geological Society Special Publication*, Vol. 10, pp. 245–258, https://doi.org/10.1144/GSL.SP.1982.010.01.16.
30. National Earthquake Study Center Team, 2017. *Peta Sumber Dan Bahaya Gempa Indonesia*. Pusat Penelitian dan Pengembangan Perumahan dan Permukiman Badan Penelitian dan Pengembangan Kementerian Pekerjaan Umum dan Perumahan Rakyat.
31. Prasetyo, H. 1992. The Bali-Flores Basin: geological transition from extensional to subsequent compressional deformation. *Proceedings Indonesian Petroleum Association Twenty First Annual Convention*, Vol. 1, pp. 455-478.
32. Satyana, A.H., Nugroho, D. and Surantoko, I., 1999. Tectonic controls on the hydrocarbon habitats of the Barito, Kutei, and Tarakan Basins, Eastern Kalimantan, Indonesia: Major dissimilarities in adjoining basins. *Journal of Asian Earth Sciences*, Vol. 17, pp. 99–122, https://doi.org/10.1016/S0743-9547(98)00059-2.
33. Satyana, A.H., 2005. Oligo-Miocene carbonates of Java, Indonesia: tectonic-volcanic setting and petroleum implications. *Proceedings, Indonesian Petroleum Association Thirtieth Annual Convention Exhibition*, pp. 217–249.
34. Simoes, M., Avouac, J.P., Cattin, R. and Henry, P., 2004. The Sumatera subduction zone: A case for a locked fault zone extending into the mantle. *Journal of Geophysical Research,* Vol. 109, No. B10402,

pp. 1-16, https://doi.org/10.1029/2003JB002958.

35. Smith, W.H.F. and Wessel, P., 1990. Gridding with continuous curvature splines in tension. *Society of Exploration Geophysicist*, Vol. 55, No.3, pp. 293–305, https://doi.org/10.1190/1.1442837.
36. Soeria-Atmadja, R., Suparka, S., Abdullah, C., Noeradi, D. and Sutanto, 1998. Magmatism in western Indonesia, the trapping of the Sumba Block and the gateways to the east of Sundaland. *Journal of Asian Earth Sciences,* Vol. 16, No. 1, pp. 1-12, https://doi.org/10.1016/S0743-9547(97)00050-0.
37. Suryanto, W., Nurdiyanto, B. dan Pakpahan, S., 2010. Implementasi Perhitungan Receiver Function Untuk Gempa Jauh (Teleseismic) Menggunakan Matlab. *Jurnal Meteorologi dan Geofisika,* Vol. 11, No. 1, hal 67-73, https://doi.org/10.31172/jmg.v11i1.64.
38. Syuhada and Anggono, T., 2016. Crustal structure in the southern part of West Java based on analysis of teleseismic receiver function. *AIP Conference Proceedings*. Vol. 1711, pp. 070001-1–070001-6 https://doi.org/10.1063/1.4941642.
39. Wicaksono, B., Setyoko,J. and Panggabean H., 2009. The North Sumatera Basin: Geological Framework & Petroleum System Review. Lemigas. <*http://www.ccop.or.th/eppm/projects/1/docs/IN_NorthSumatera_ccop_2009krabi.pdf*>.
40. Wölbern, I. and Rümpker, G., 2016. Crustal thickness beneath Central and East Java (Indonesia) inferred from P receiver functions. *Journal of Asian Earth Sciences*, Vol. 115, pp 69–79, https://doi.org/10.1016/j.jseaes.2015.09.001.
41. Zhu, L. and Kanamori, H., 2000. Moho depth variation in southern California. *Journal of Geophysical Research*, Vol. 105, No. B2, pp. 2969–2980, https://doi.org/10.1029/1999JB900322.

Tables

Table 1. Comparison of sediment and Moho depth in Sumatera from different studies

Station	Sediment thickness (km)	Moho depth (km)	References
GSI	5	40	Kieling et al. (2011)
	4	30	Macpherson et al. (2012)
	3	19	Bora et al. (2016)
	6	38	Present study
BKNI	1	30	Macpherson et al. (2012)
	1	27-30	Bora et al. (2016)
	2	46	Present study
LHMI	5	19	Macpherson et al. (2012)
	7	35	Bora et al (2016)
	8	34	Present study
MNAI	2	16	Macpherson et al. (2012)
	4	31	Bora et al (2016)
	2	20	Present study
PMBI	1	32	Bora et al. (2016)
	2	50	Present study
PSI	1	33	Kieling et al. (2011)
	2	40	Present study

Tabel 2. Comparison of sediment and Moho depth in West Java from different studies

Station	Sediment thickness (km)	Moho depth (km)	References
JCJI	2	30	Anggono et al. (2020)
	2	16	Present study
TNG	1	29	Anggono et al. (2020)
	2	26	Present study
CGJI		37,2	Syuhada and Anggono (2016)
	1	34	Anggono et al. (2020)
	2	36	Present study
CBJI	1	34	Anggono et al. (2020)
	6	34	Present study
DBJI	2	37	Anggono et al. (2020)
	2	20	Present study
LEM	1	32	Anggono et al. (2020)
	2	36	Present study
CNJI		35,3	Syuhada and Anggono (2016)
	1	32	Anggono et al. (2020)
	2	38	Present study
CISI		31,9	Syuhada and Anggono (2016)
	1	32	Anggono et al. (2020)
	2	46	Present study
CMJI		34,5	Syuhada and Anggono (2016)
	1	37	Anggono et al. (2020)
	2	38	Present study
SKJI		33,6	Syuhada and Anggono (2016)
	1	29	Anggono et al. (2020)
	2	20	Present study
SBJI	1	30	Anggono et al. (2020)
	2	46	Present study

Figures

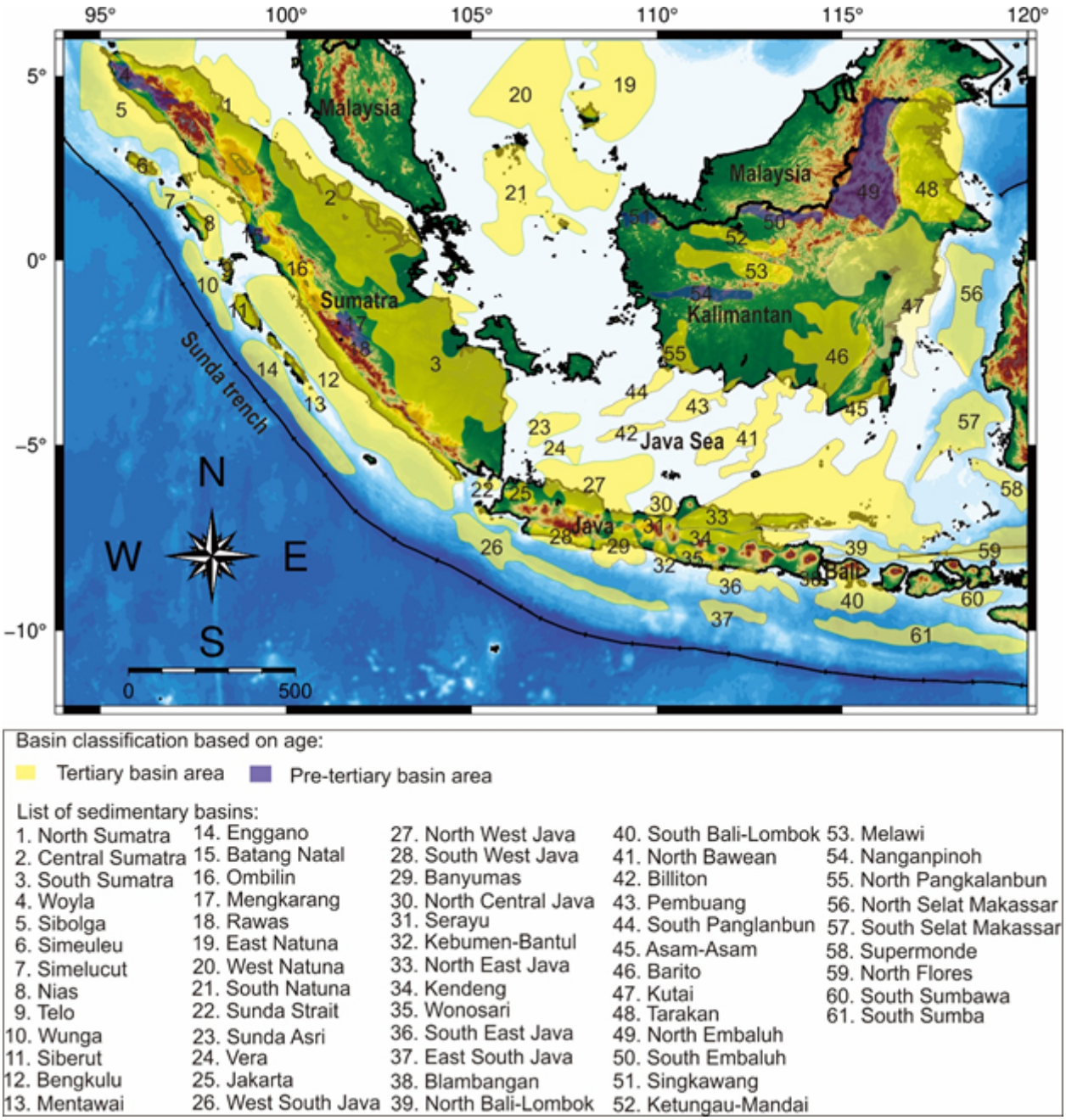

Figure 1

Sedimentary basin map of western Indonesia (from Badan Geologi (2009)). Note: The designations employed and the presentation of the material on this map do not imply the expression of any opinion whatsoever on the part of Research Square concerning the legal status of any country, territory, city or area or of its authorities, or concerning the delimitation of its frontiers or boundaries. This map has been provided by the authors.

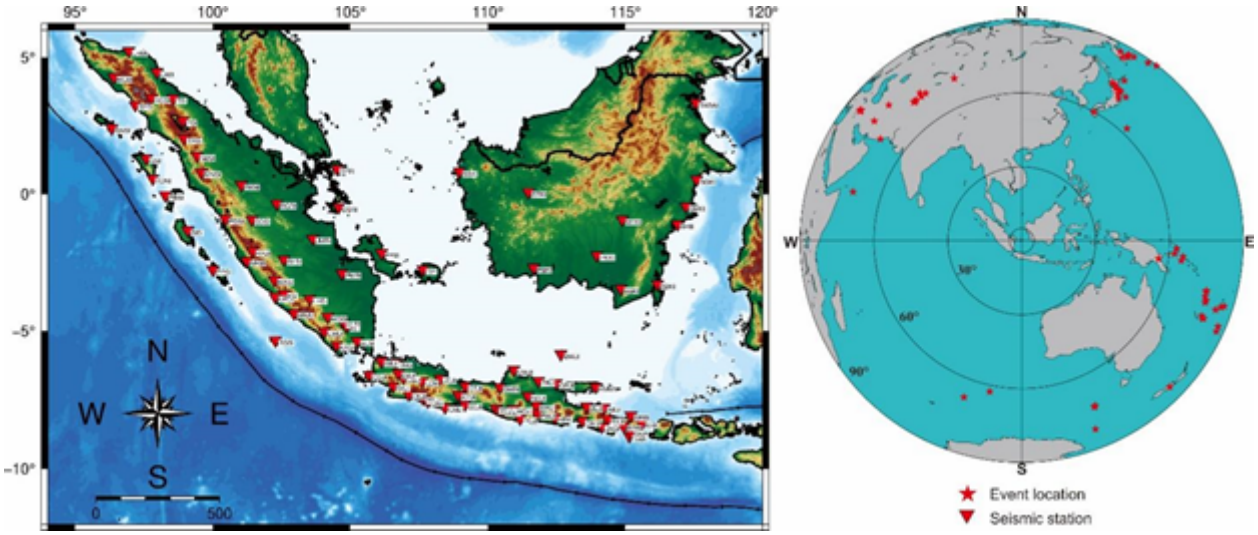

Figure 2

Location of the IA stations in Western Indonesia. Teleseismic events used to calculate the receiver functions are shown in the upper right inset. Note: The designations employed and the presentation of the material on this map do not imply the expression of any opinion whatsoever on the part of Research Square concerning the legal status of any country, territory, city or area or of its authorities, or concerning the delimitation of its frontiers or boundaries. This map has been provided by the authors.

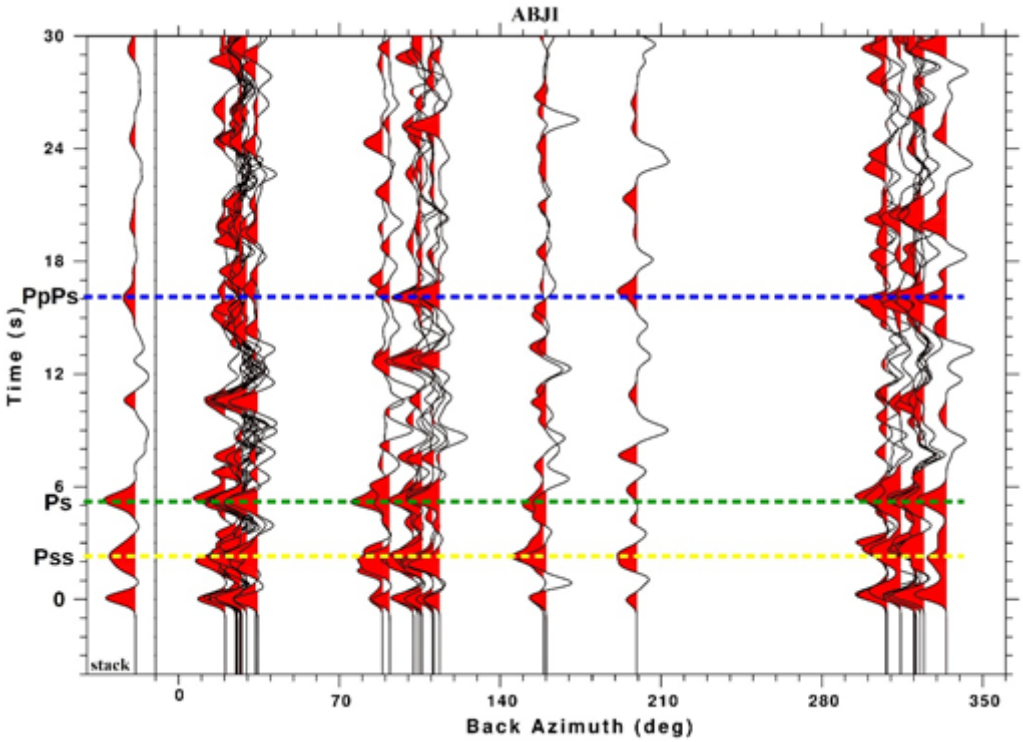

Figure 3

Radial receiver functions plotted with increasing back azimuth for station ABJI. Pss Sediment is marked in yellow, Ps Moho is marked by green dashed line, and PpPs marked by a blue dashed line.

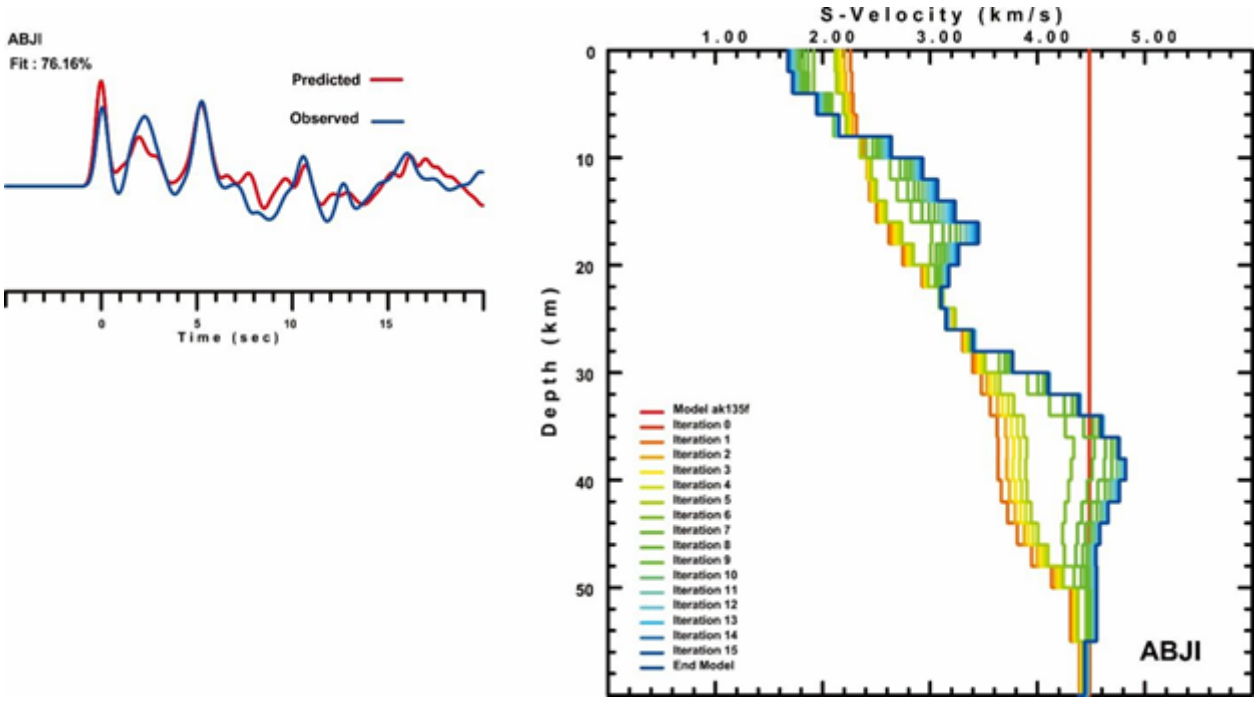

Figure 4

The inversion results obtained for station ABJI.

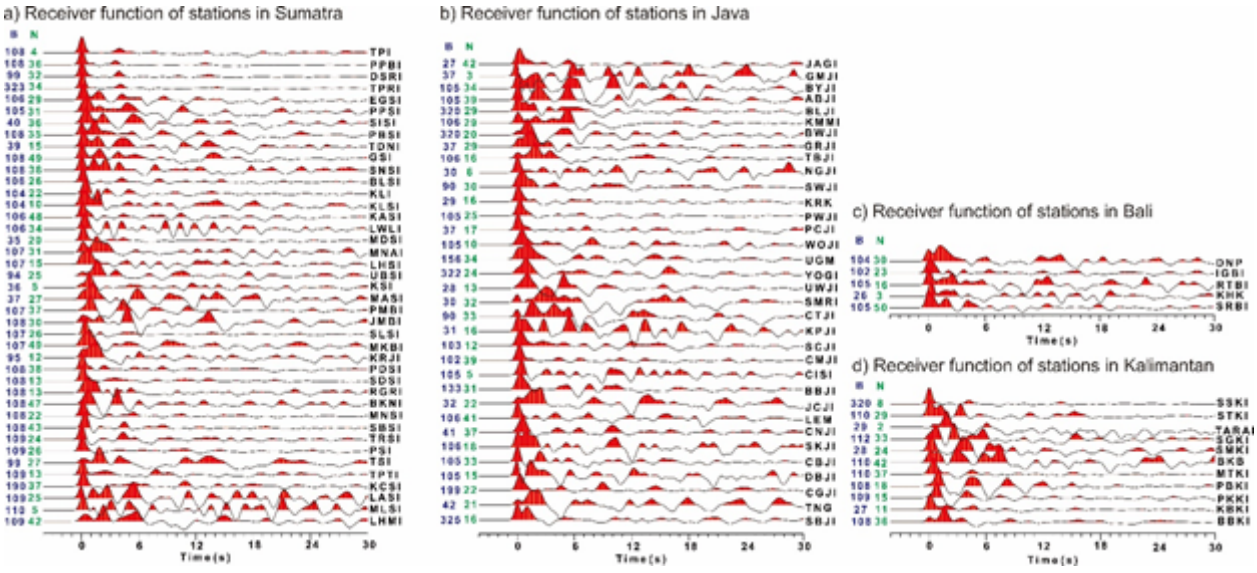

Figure 5

The plot of stacked receiver functions from different stations and Island of Sumatera (a) Java (b) Bali (c) and Kalimantan (d). Average back azimuth (B in degrees, blue colour) and the number of receiver functions (N, green colour) for each station.

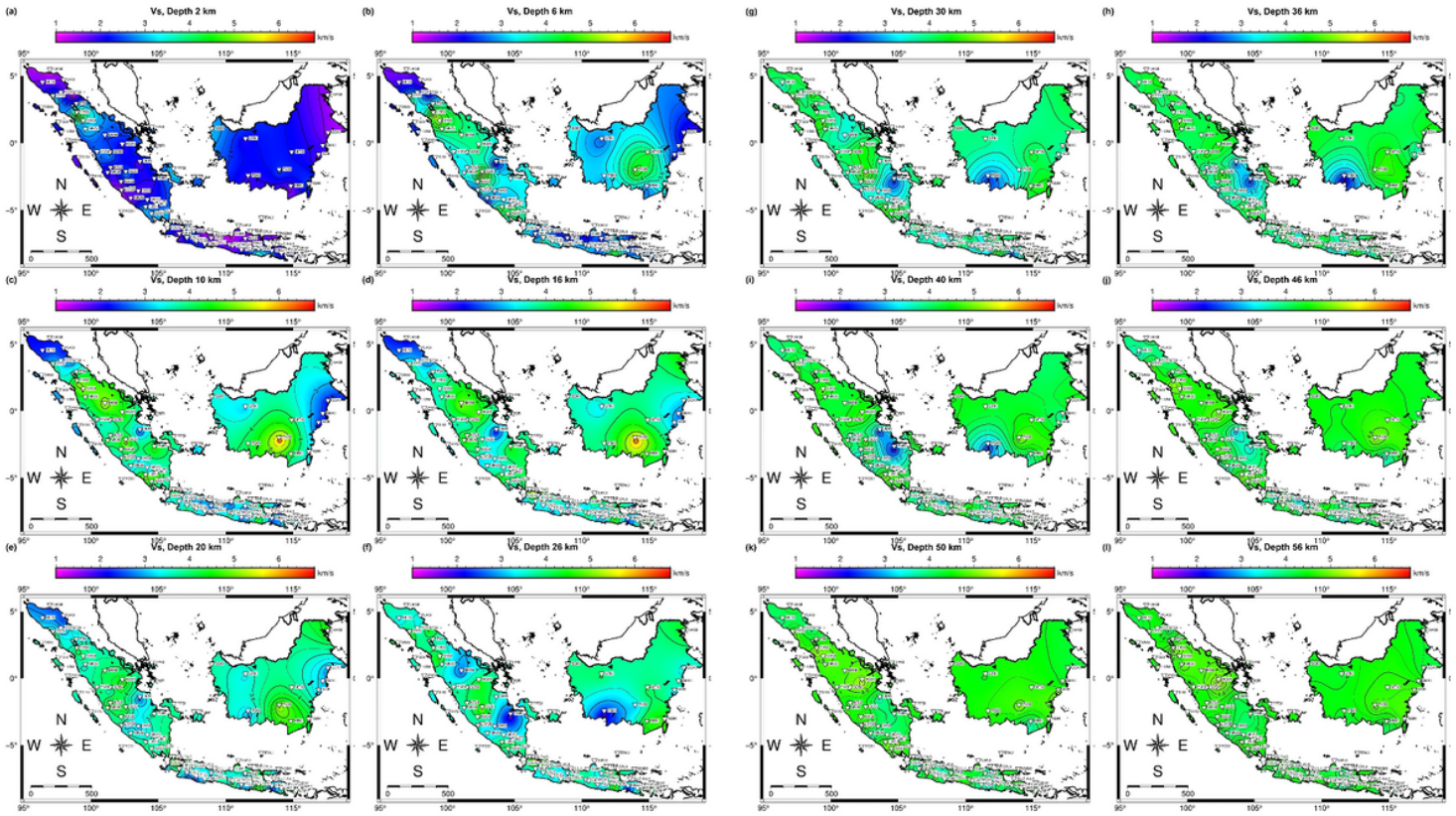

Figure 6

Map of the distribution of S-wave velocity on variations in the depth of the earth under Western Indonesia. (a) 2 km, (b) 6 km, (c) 10 km, (d) 16 km, (e) 20 km, (f) 26 km, (g) 30 km, (h) 36 km, (i) 40 km, (h) 46 km, (k) 50 km, (l) 56 km, (m) 50 km, (n) 56 km. The white symbol represents the position of the BMKG station. Note: The designations employed and the presentation of the material on this map do not imply the expression of any opinion whatsoever on the part of Research Square concerning the legal status of any country, territory, city or area or of its authorities, or concerning the delimitation of its frontiers or boundaries. This map has been provided by the authors.

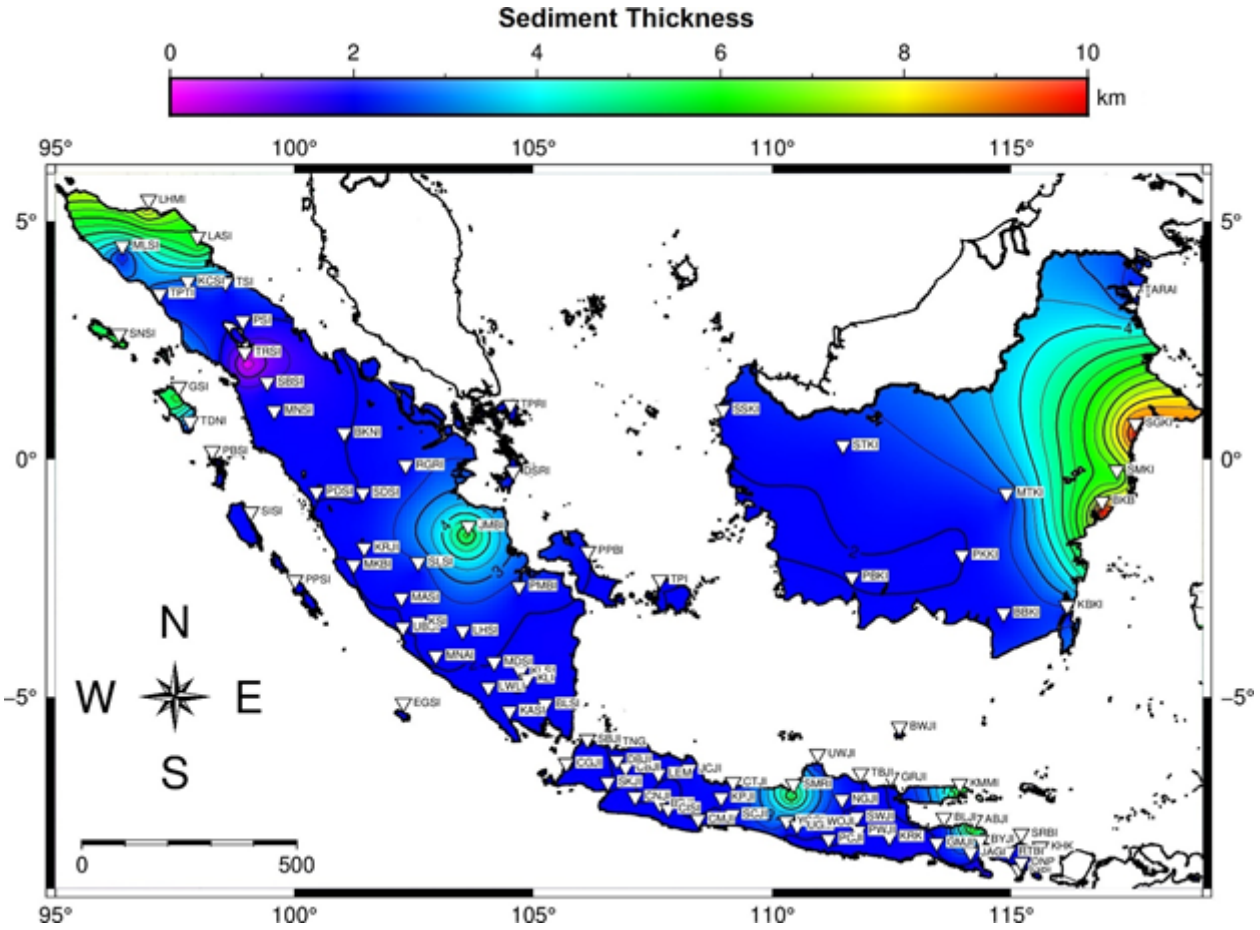

Figure 7

Map of variations in sediment thickness in Western Indonesia. The white symbol represents the position of the BMKG station. Note: The designations employed and the presentation of the material on this map do not imply the expression of any opinion whatsoever on the part of Research Square concerning the legal status of any country, territory, city or area or of its authorities, or concerning the delimitation of its frontiers or boundaries. This map has been provided by the authors.

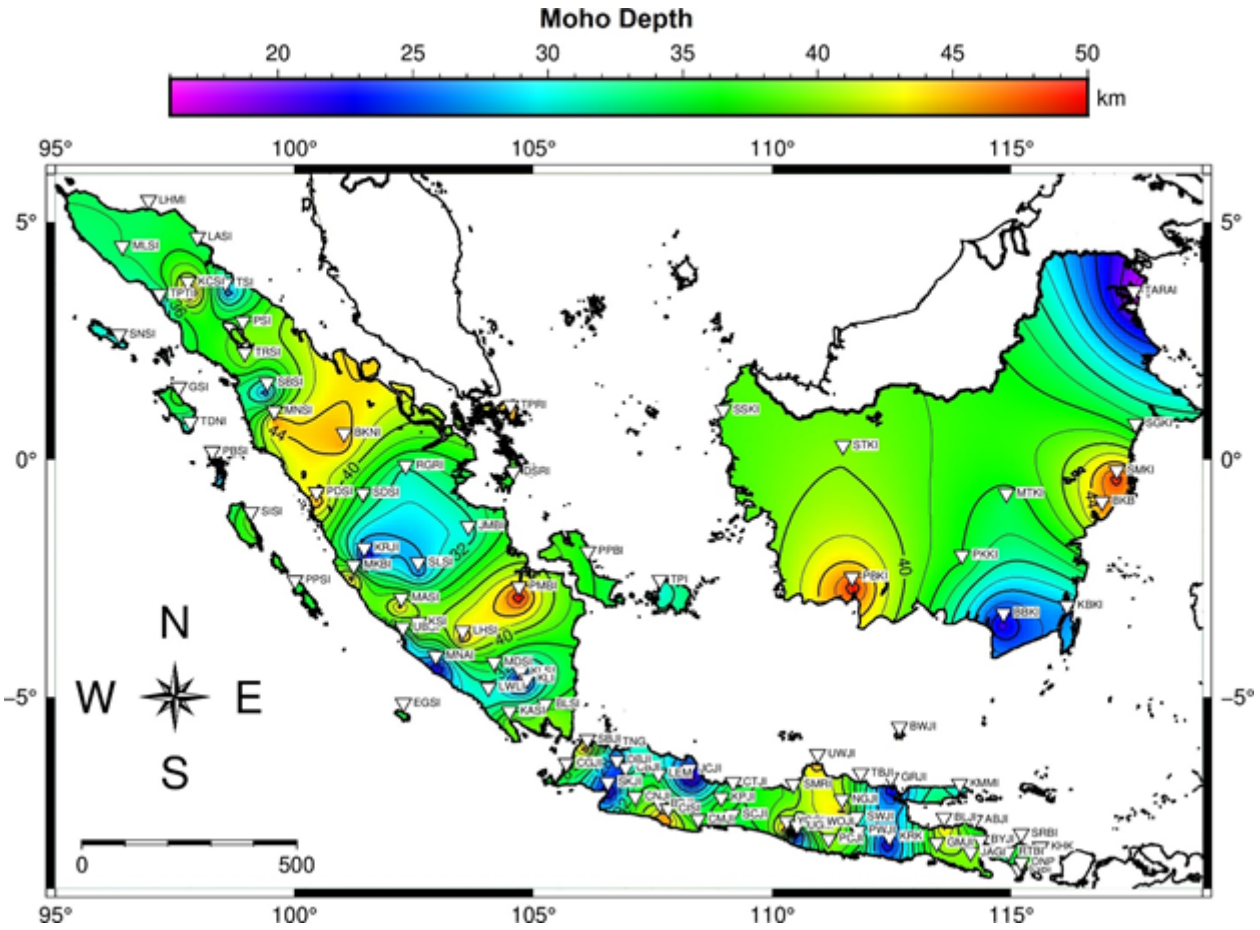

Figure 8

Map of variations Moho depth in Western Indonesia. The white symbol represents the position of the BMKG station. Note: The designations employed and the presentation of the material on this map do not imply the expression of any opinion whatsoever on the part of Research Square concerning the legal status of any country, territory, city or area or of its authorities, or concerning the delimitation of its frontiers or boundaries. This map has been provided by the authors.

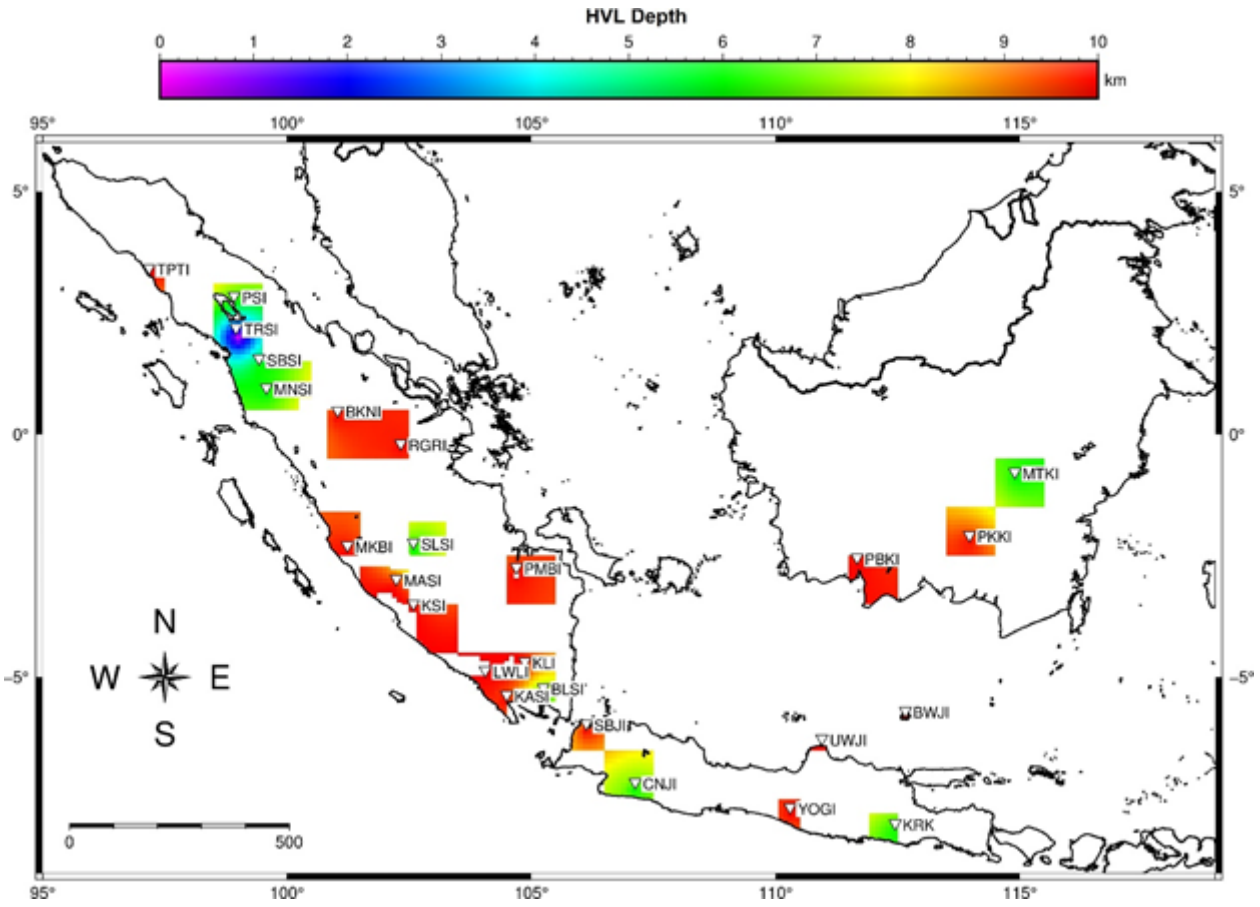

Figure 9

Map of HVL depth distribution under stations in Western Indonesia. The white symbol represents the position of the BMKG station. Note: The designations employed and the presentation of the material on this map do not imply the expression of any opinion whatsoever on the part of Research Square concerning the legal status of any country, territory, city or area or of its authorities, or concerning the delimitation of its frontiers or boundaries. This map has been provided by the authors.

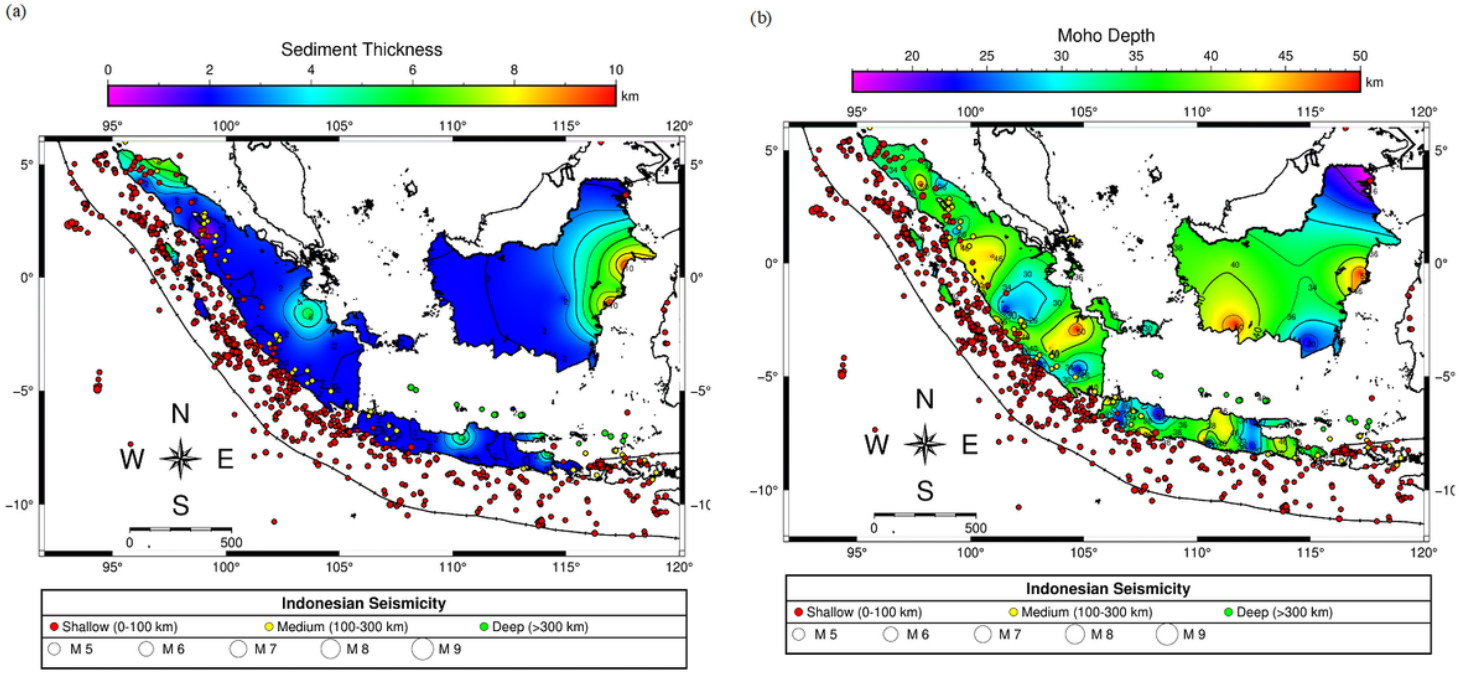

Figure 10

Earthquake distribution maps for Mw> 5.0 during 2010-2020 which correlate with (a) variations in sediment thickness and (b) variations in Moho depth in western Indonesia. Note: The designations employed and the presentation of the material on this map do not imply the expression of any opinion whatsoever on the part of Research Square concerning the legal status of any country, territory, city or area or of its authorities, or concerning the delimitation of its frontiers or boundaries. This map has been provided by the authors.